Original Research Article

# Automatic detection of tuberculosis bacilli from microscopic sputum smear images using deep learning methods

Rani Oomman Panicker [a,c,*], Kaushik S. Kalmady [b], Jeny Rajan [b], M.K. Sabu [c]

[a] Department of Information Technology, College of Engineering, Trikaripur, Kerala, India
[b] Department of Computer Science and Engineering, National Institute of Technology Karnataka, Surathkal, India
[c] Department of Computer Applications, Cochin University of Science and Technology, Kochi, India

ARTICLE INFO

ABSTRACT

An automatic method for the detection of Tuberculosis (TB) bacilli from microscopic sputum smear images is presented in this paper. According to WHO, TB is the ninth leading cause of death all over the world. There are various techniques to diagnose TB, of which conventional microscopic sputum smear examination is considered to be the gold standard. However, the aforementioned method of diagnosis is time intensive and error prone, even in experienced hands. The proposed method performs detection of TB, by image binarization and subsequent classification of detected regions using a convolutional neural network. We have evaluated our algorithm using a dataset of 22 sputum smear microscopic images with different backgrounds (high density and low-density images). Experimental results show that the proposed algorithm achieves 97.13% recall, 78.4% precision and 86.76% F-score for the TB detection. The proposed method automatically detects whether the sputum smear images is infected with TB or not. This method will aid clinicians to predict the disease accurately in a short span of time, thereby helping in improving the clinical outcome.

© 2018 Nalecz Institute of Biocybernetics and Biomedical Engineering of the Polish Academy of Sciences. Published by Elsevier B.V. All rights reserved.

## 1. Introduction

Tuberculosis (TB) is a potentially serious contagious infection and is caused by Mycobacterium tuberculosis. It is an airborne disease that spreads from one person to another through coughs, sneezes, speaks, spits etc. and it predominantly attacks the lungs (pulmonary TB). But it can also infect or damage other organs (extrapulmonary TB) such as the brain, spine, kidney etc. and may eventually lead to death, if not handled properly. These bacteria are rod-shaped, slow growing with varying curvature and have a length ranging from 1 to 10 μm [9]. Depending upon the level of infection, doctors classified TB into two forms: active TB and latent (inactive) TB. Among them, active TB is more dangerous and is contagious. Patients with latent TB do not spread infection, but sometimes it can be converted to active TB at a later stage.

Based on the report of World Health Organization (WHO) 2017 [1], in 2016 itself, 1.3 million people died and an estimated 10.4 million fell ill due to TB. Top TB burden countries include India, Indonesia, China, Pakistan etc., and among these countries, India (25%)is having the maximum population of TB patients [1]. Every year millions of people worldwide are affected with TB infection, leading to WHO announcing TB as a global emergency [2].

There are many established TB detection methods available such as microscopy, tuberculin skin test (TST), chest X-ray, interferon-γ release assay (IGRA), culture test, and GeneXpert etc. [3]. However, microscopic sputum smear examination using conventional microscope is a widely used technique all over the world especially in low and middle-income countries due to its low cost, ease of use and maintenance; and also provides sufficiently faster results compared to other tests [3]. Sputum smear examination can be done in two ways: one with the help of bright field or conventional microscope and the other with the help of a fluorescent microscope, and both of them vary in their power of the lens and staining. Former one uses $100\times$ lens and Ziehl-Neelsen (ZN) acid-fast staining procedure and the latter one uses $25\times$ and auramine-O [4].

Accurate and on time treatments are required for controlling the number of TB cases. Manual detection and counting of TB bacilli through the microscopic eyepiece is a tedious task, which requires highly skilled lab technicians, and lots of mental and physical (eye) strain [3]. The accuracy of TB detection always depends upon the technician's level of expertise and knowledge. Technicians, in general, have to analyze between 20 and 100 fields of each sputum smear slide, which can take about 40 min to 3 h depending upon the patient's infection level [6]. According to Veropoulos et al. [7], the manual TB detection and counting methods may miss 33–50% of active cases and the automated methods may help to increase the diagnostic sensitivity rate, as machines can screen a large number of fields in a short duration and can detect the TB bacillus more accurately in the early stage itself. The other advantages of automated TB detection methods are low mental and physical strain, faster and accurate decision making, patient record use, multi-head visualization and communication use (second opinion) [10]. The usage of these types of automated systems and methods will help the clinicians to provide better treatments to the needy and thereby the hospitals can meet the quality standards.

In the past few years, many automated methods have been proposed to detect TB bacilli from conventional as well as fluorescence microscopic images. Most of the existing methods use handcrafted feature vectors to discriminate bacilli pixels from non-bacilli pixels. The performance of these methods heavily depends on the bacilli features considered. Also, manually designing feature vectors for complex tasks requires a great deal of human time and effort [31]. In this work, we used a customized convolutional neural network (CNN) to identify the pixels in the image that belongs to bacilli. The advantage of CNN over other machine learning techniques is that instead of handcrafted feature vectors, the CNN automatically learns the characteristics of bacilli, provided enough samples to learn. We used a standard dataset provided by Costa et al. [27] to train and test the proposed CNN framework.

This paper is structured as follows. Section 2 describes the review of existing papers. In Section 3, the proposed methods are discussed. Experimental results, data sets, and discussions are given in Section 4. Finally, conclusions are drawn in Section 5.

## 2. Related work

Many researchers proposed fully and semi-automatic TB bacilli detection methods for sputum smear images acquired using a conventional or fluorescent microscope. The general steps involved in developing automated systems for TB bacilli detection are: (i) image acquisition and pre-processing, (ii) segmentation, (iii) feature extraction, and (iv) classification of TB bacilli. The first attempt to detect TB bacilli from microscopic sputum smear images using image processing techniques was done by Veropoulos et al. [8] in 1998. They demonstrated the efficacy of their method on images acquired with a fluorescent microscope. Costa et al. [5] were the first to publish bacilli detection using image processing techniques on bright field microscopic images. In the remaining part of this section, we will be discussing automatic TB detection methods using conventional microscopic images only.

Costa et al. [5] proposed an adaptive thresholding-based segmentation method for the detection of TB in images of ZN-stained sputum smear images. They used morphological filters for handling the artifacts. But the sensitivity of their method was relatively less (76.65%). In 2008 itself, Sadaphal et al. [11] used Bayesian segmentation and shape features (axis ratio and eccentricity) for the detection of TB bacilli. However, their method failed in identifying the overlapping or conglomerated bacilli. An adaptive hue based segmentation method was later proposed by Makkapati et al. [12] in 2009, for detecting TB bacilli. In [13], a thresholding-based segmentation was used by considering Cr and a plane of YCbCr and Lab color space for the identification of bacilli from sputum smear images. They got an accuracy of 85.7%. Zhai et al. [14] proposed a two-stage segmentation (coarse segmentation and fine segmentation) and a decision tree based classification for TB bacilli identification, and their experimental results showed an accuracy greater than 80%. In the same year itself, Nayak et al. [15] proposed HSI color space based segmentation and area-based classification for detecting TB bacilli with 93.5% success rate. A genetic algorithm based neural network (GA-NN) approach has been used for the detection of TB objects and an accuracy of 86.32% has been reported on ZN stained tissue slide images [19].

A pixel classifier combination is used for detecting TB bacilli in [9,16]. These methods failed to identify touching TB bacilli. In 2012, Costa Filho et al. [17] performed a neural network-based classification for detecting TB bacilli with a sensitivity of 91.53%. A Random Forest (RF) based learning method was proposed by Ayas et al. [18] in 2014 for detecting TB bacilli. Recently, in 2015 Costa Filho et al. [20] used segmentation and post-processing method for the automatic identification of TB. The authors achieved a sensitivity of 96.80%. Very recently, a fuzzy-based decision-making approach was developed

by Ghosh et al. [22]. In this method, they segmented the bacilli using shape, color and granularity feature. They used gradient based region growing technique for finding the contour boundary. However, their method failed to identify overlapping bacillus. In 2017, Lopez et al. [28] proposed a CNN model for identifying TB bacilli from sputum smear images. They used RGB, grayscale and R-G patches versions for training the 3 CNN models.

Generally, a TB dataset image consists of three types of objects such as single bacilli, touching or overlapping bacilli, and debris. Although the touching bacilli are composed of several single bacillus objects that are touched together in different ways, its inclusion is very important for determining the severity of the TB disease. But most of the abovementioned papers [9,16,20] concentrate on the segmentation of single bacilli objects only. They either discard or consider the touching bacilli as non-bacillus objects due to their irregular shapes. According to Panicker et al. [3], most of the automated methods proposed in the literature failed in detecting touching bacillus objects. In [9,16] the authors suggested that the touching bacillus objects formed a T shape and are labeled as non-bacillus objects. According to Xu et al. [21], the touching bacilli is considered as another class of objects or negative ones. The extraction of single bacilli and touching TB bacilli is a very important problem in the clinical context for deciding the infection level.

## 3. Methods

The proposed method is implemented in two stages. In the first stage, we used a simple segmentation approach to classify the foreground and background of the images. The foreground consists of single bacilli, touching bacillus and other artifacts. The segmented foreground objects are then given to a trained convolutional neural network (CNN) and the CNN will classify the objects into bacilli and non-bacilli. Both sections are explained in detail in the following subsections.

### 3.1. Stage – 1: Image binarization

In the first stage, the input image is first denoised to improve the quality. In this work, we used the fast nonlocal means (FNLM) method [29] to denoise the images. The parameters used for FNLM are: smoothing parameter = 3, search window size = 25 × 25, similarity window size = 5 × 5. The denoised image is then binarized using Otsu's method [30] after converting the image to grayscale. The binarization threshold value estimated using the Otsu's method will classify the pixels in the given grayscale image to background and foreground. The background pixels will be represented with zero and foreground with one. The foreground region will contain bacilli as well as some other foreign objects. Morphological opening and closing are applied to the resultant binary image to fine tune it. A connected component analysis is applied to the binary image to extract all the connected components and the extracted connected components (after multiplying with the original image) will be fed into the second stage to check whether the connected component is a bacillus or not. A sample input and output of the first stage is given in Fig. 1. Fig. 1a–c shows the original input image, denoised image and the output of stage 1 respectively. The selected patches in Fig. 1c are the regions selected as bacillus by the stage 1 process. These regions may also contain debris, stains or noise. These patches will be fed to stage 2 for further
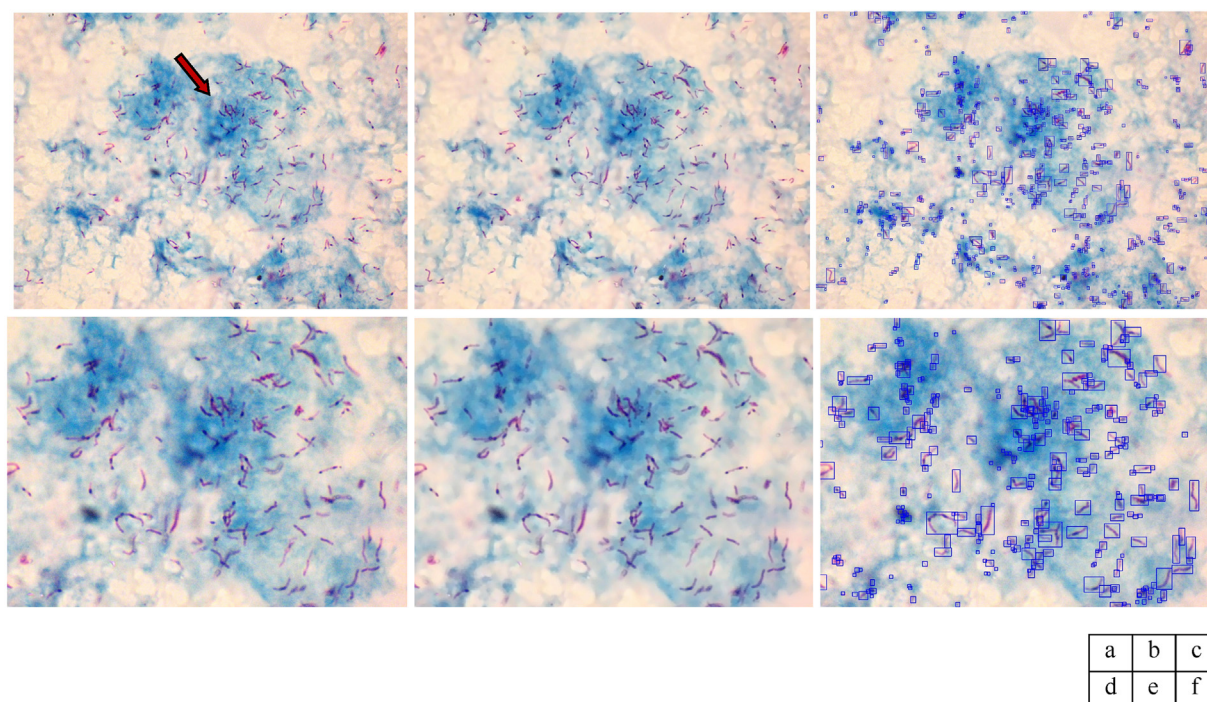


| a | b | c |
| d | e | f |

**Fig. 1 – Results of stage-1. (a) Original image, (b) denoised image, (c) selected objects after binarization and connected component analysis. The images in the second row, (d), (e), and (f) are the zoomed view of the region with red arrow in image (a).**

processing. The images in the second row of Fig. 1 are the zoomed view of the region with a red arrow in Fig. 1a.

### 3.2. Stage – 2: Pixel classification

A convolutional neural network (CNN) is used in stage 2 to verify whether the extracted patch in stage 1 is a bacillus or

not. The CNN architecture proposed for the second stage is described in Fig. 2.

#### 3.2.1. Network architecture
The proposed CNN model accepts an image patch (from stage 1) as input and generates a probability value that is used to predict whether the given input patch contains bacilli or not.
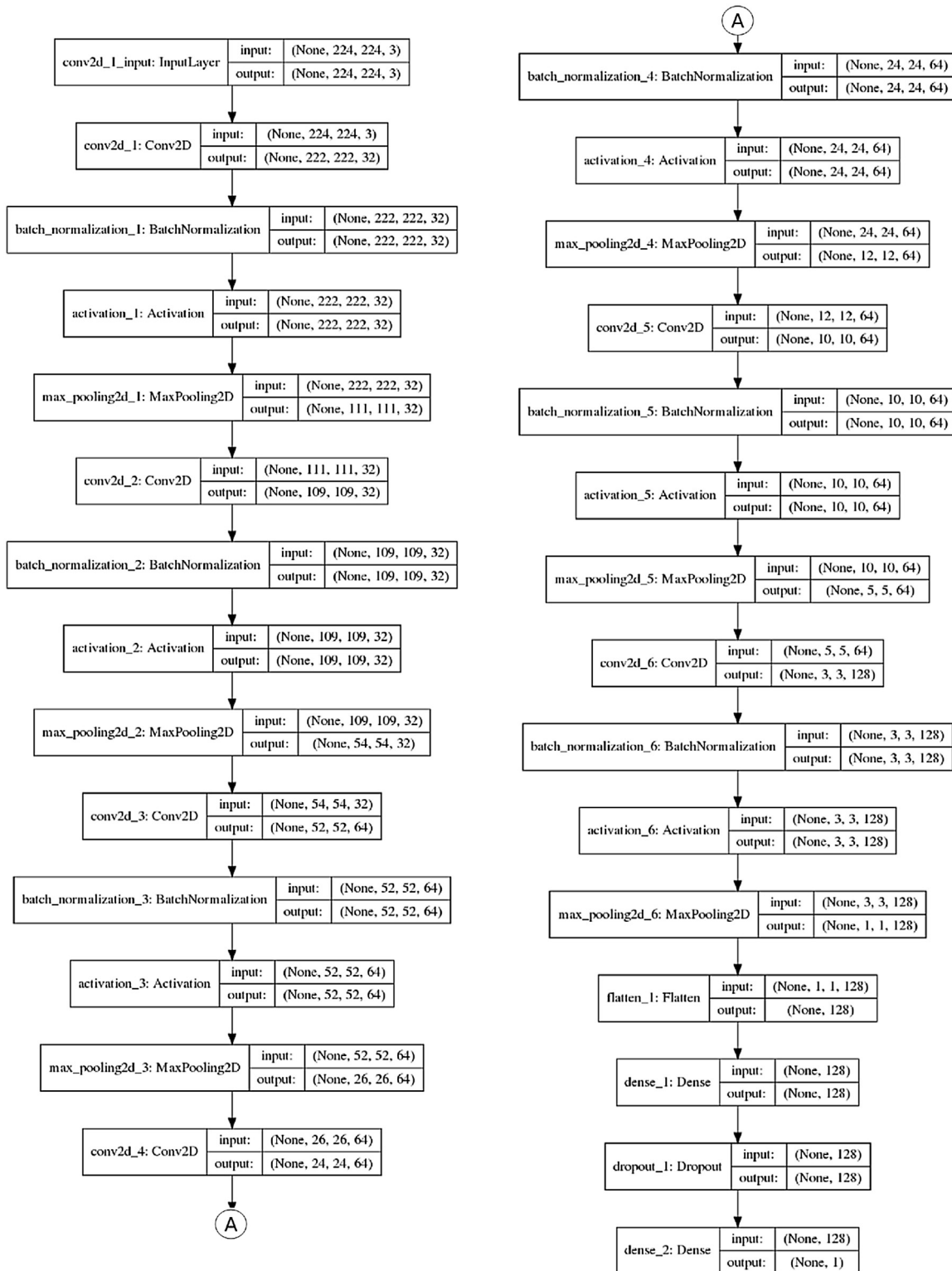


**Fig. 2 – Proposed CNN architecture.**

As shown in Fig. 2, the final architecture consists of 2 convolution layers with 32 (3 × 3) filter maps followed by 3 convolution layers with 64 (3 × 3) filters and finally 1 convolution layer with 128 (3 × 3) filters. The output from this series of convolution layers is fed to a fully connected layer with 128 neurons with Rectified Linear Unit (ReLU) activation and finally a sigmoid neuron for binary classification. The ReLU and sigmoid activation functions are defined as:

$$f(a) = \max(a, 0) \tag{1}$$

and

$$\sigma(a) = \frac{1}{1 + e^{-a}} \tag{2}$$

respectively, where $a$ is the weighted sum of the inputs.

Each convolution layer is followed by a Batch Normalisation Layer [23]. Batch Normalization is a technique used to reduce the internal covariate shift and has been observed to increase the speed of training of neural networks. As a result, the output from the convolution layer is whitened to have zero mean and unit variance before being fed as input to the next layer. Every Batch Normalisation Layer is followed by a ReLU Activation function which suppresses the value if it is negative. CNN's with ReLU activation units are observed to train faster than their equivalent networks with the standard tanh activations [24]. Max pooling usually follows the ReLU Activation layer. In our experiments, we use max pooling tiles of 2 × 2 pixels. During max pooling, the feature map obtained after the application of the ReLU activation function on the output of the convolution block is divided into 2 × 2 tiles and the maximum value from each tile is used in the next layer of the network. Additionally, the fully connected layer is followed by a dropout layer having probability 0.5 to further reduce overfitting.

### 3.3. Training methodology

We incrementally added convolution layers to check for improvement in validation accuracy until the final configuration is reached. The loss function that we used in the proposed model is the binary cross entropy function:

$$L = -\sum_{i=1}^{n} (t_i \log(y_i) + (1 - t_i) \log(1 - y_i)) \tag{3}$$

where $L$ is the loss function, $n$ is the input size $t_i$ is the actual binary output and $y_i$ is the estimated binary output. The objective is to find the parameters (weight and bias vectors) that minimize the loss function. We train the network using the Gradient Descent method with a learning rate of 0.01. The weights are initialized using the Glorot uniform initializer as per the default parameters in the Keras API. It randomly draws

samples from a uniform distribution as per configurations describes in [25]. All images are scaled to a fixed size of 224 × 224 before being fed as input to the model. We used the resize function (with nearest-neighbor interpolation) in the Python Imaging Library to resize the input images. The inputs are whitened – i.e., linearly transformed to have zero means and unit variances in each of the RGB channels, as this has proven to enable faster convergence in network training [26]. We further curb over fitting and improve the robustness of the model using data augmentation techniques (by adding vertical and horizontal reflections, rotation of 180 degrees of images in the training set and extend the number of training samples). This provided a significant improvement in model performance, increasing the test accuracy by 5%. The network is trained for 75 epochs with a batch size of 32. Fig. 4 shows the training and validation loss (and accuracy) for the 3 different models that were trained.

## 4. Experimental results and discussion

### 4.1. Dataset

We conducted experiments on the public dataset provided by Costa et al. [27]. The dataset of TB images was prepared at the INPA (Instituto Nacional de Pesquisas da Amazonia) lab, Manaus, Brazil. The images were captured using Canon Power Shot A640-10 megapixel digital camera and a 100× Zeiss Axioskope-4 microscope with 1.25 numerical aperture. The image database consists of 120 images and their ground truths, each of them are in 2816 × 2112 pixel resolution [27,32]. All ground truth images are marked by different shapes such as circle represents single bacilli, rectangle represents agglomerated bacilli or touching bacilli and polygon represents doubtful bacilli [27]. The dataset contains both high density (TB-HDB) and low-density background (TB-LDB) images. i.e., the strong and weak presence of methylene blue counter stain shows prevalent blue color for TB-HDB images and prevalent white color for TB-LDB images [27,32]. In this study, we used both types of images for experimental analysis and considered only single bacilli and agglomerated bacilli for measuring the performance due to the reason that clinicians always determine the infection level based on these two bacillus objects.

### 4.2. Results

#### 4.2.1. Training result

For training and testing the proposed CNN, we cropped 900 positive patches and 900 negative patches from images with different backgrounds from the aforementioned database. Sample positive and negative patches are shown in Fig. 3. Out of 1800 patches, 80% were used for training and 20% were used
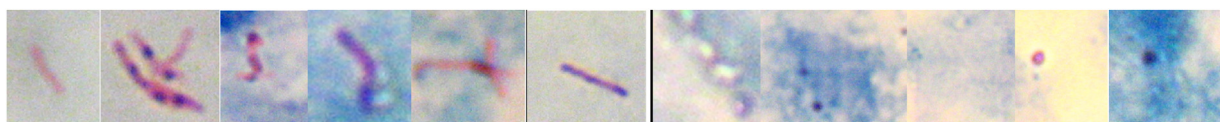


**Fig. 3 – Samples patches used for training and testing. Patches with bacilli as well as debris and background can be seen in the figure.**
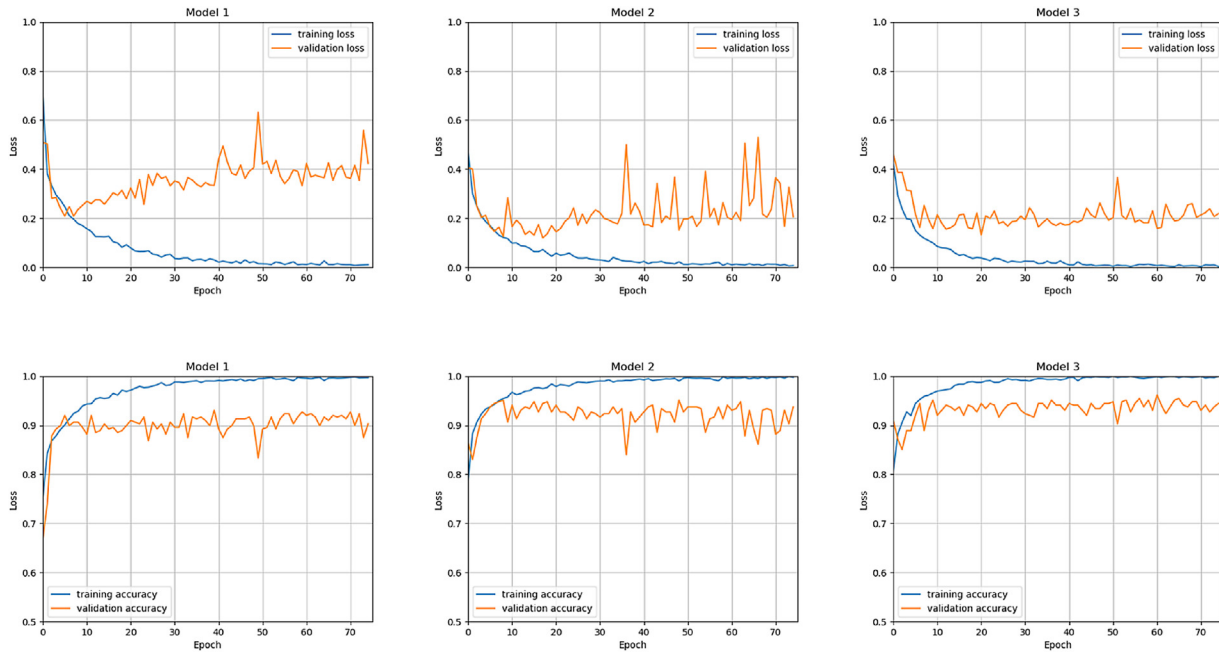
**Fig. 4 – Row-1: Training and validation loss for model 1, model 2 and model 3 for 75 epochs. Row-2: Training and validation accuracy for model 1, model 2 and model 3.**

as test set. For validation, 20% of images from training set were used. We begin with CNN architecture consists of 2 convolution layers with 32 (3 × 3) kernels and 1 convolution layer with 64 (3 × 3) kernels followed by a fully connected layer of 128 neurons and a sigmoid output layer. We then incrementally add convolution layers and retrain the network until convergence in validation accuracy is achieved, resulting in the final architecture as described in the earlier sections. The training and validation loss (for 75 epochs) and training and validation accuracies for all the three models are plotted in Fig. 4. The testing accuracies for each of the incremental models are described in Table 1. All of the experiments were run on NVIDIA Quadro M2000 GPU with 4GB memory running Anaconda with Python 3.

*4.2.2. Segmentation results and discussions*
Segmentation results of the proposed method are compared with manually detected ground-truth provided with Costa et al. [27]. For the analysis, we used 22 images with different backgrounds from the database. We calculated True Positives, False Positives and False Negatives. True Positives (TP) are defined as number of true TB bacilli detected by the algorithm, False Positives (FP) are defined as total number of non-bacilli

identified as bacilli by the algorithm, and False Negatives (FN) are defined as the number of true TB bacilli that are not detected by the algorithm. We then calculate widely used performance metrics such as Recall/Precision and F-score for validating our experimental results. These metrics are widely used in the field of computer vision and medicine for determining performance.

$$\text{Precision} = \frac{\text{TP}}{\text{TP} + \text{FP}} \tag{4}$$

$$\text{Recall} = \frac{\text{TP}}{\text{TP} + \text{FN}} \tag{5}$$

$$F\text{-score} = 2 * \frac{\text{Precision} * \text{Recall}}{\text{Precision} + \text{Recall}} \tag{6}$$

To reduce false positives and computational time, we ignored patches (from stage-1) with very small sizes. i.e., these patches where both the height and the width are less than 10 pixels (threshold = 10). These small patches will not be fed to the CNN for further analysis. Table 2 shows the results

| Table 1 – Testing accuracies of the proposed model. | |
| --- | --- |
| Model architecture | Test accuracy |
| Model 1:<br>2 × (32 3 × 3 conv) + 1 × (64 3 × 3 conv) + fc (128 neurons) + output(sigmoid) | 97.21% |
| Model 2:<br>2 × (32 3 × 3 conv) + 3 × (64 3 × 3 conv) + fc (128 neurons) + output(sigmoid) | 98.32% |
| Model 3:<br>2 × (32 3 × 3 conv) + 3 × (64 3 × 3 conv) + 1 × (128 3 × 3 conv) + fc (128 neurons) + output(sigmoid) | 98.88% |

### Table 2 – Precision and recall with and without threshold.

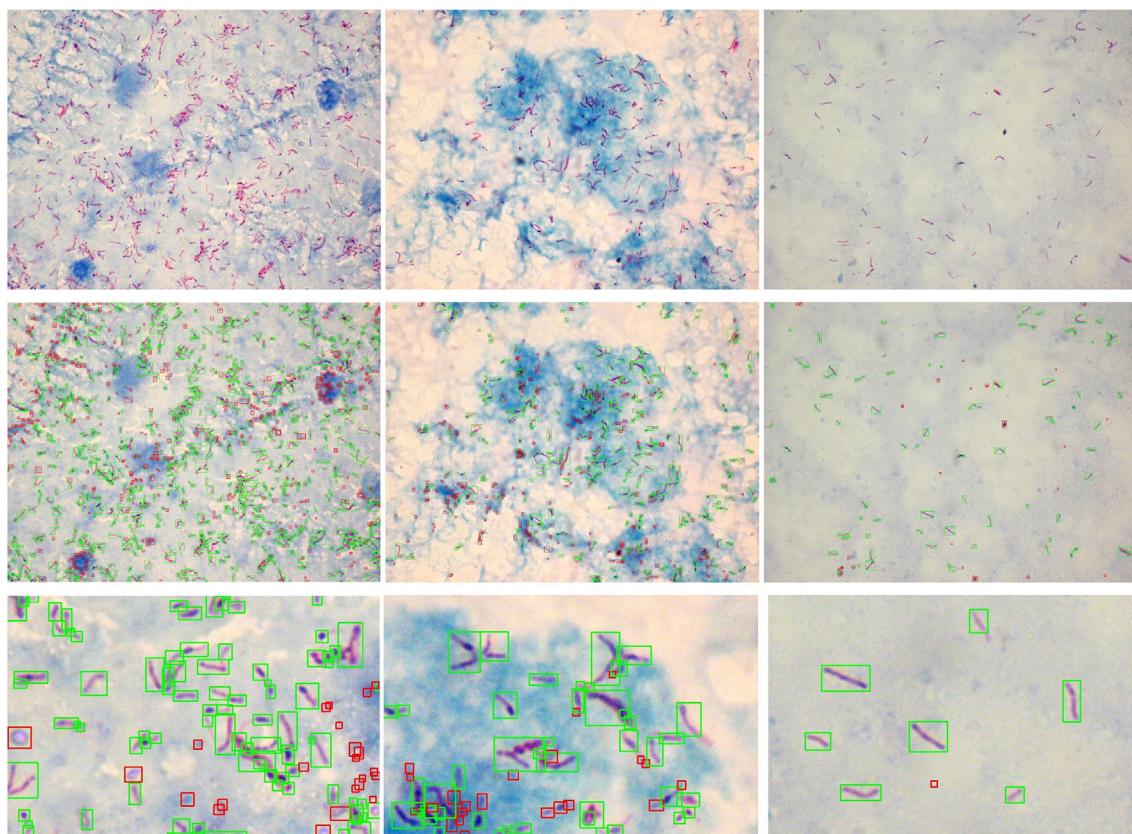| Results | No threshold | Threshold = 10 |
| --- | --- | --- |
| Precision | 78.02% | 78.4% |
| Recall (sensitivity) | 97.13% | 97.13% |
| F-score | 86.53% | 86.76% |

(Precision, Recall and F-Score) with and without threshold. Precision and Recall are computed region wise (object wise). For visual analysis, the final results on selected images are shown in Fig. 5. The boxes in the resultant image show the objects detected in stage-1 and in stage-2 these objects will be classified as bacilli and non-bacilli objects. The objects in green boxes are classified as bacilli by the proposed CNN and the objects in red boxes are classified as non-bacilli objects.

We also compared our results with Costa Filho et al. [20] due to the reason that they used the same database for experimental analysis. They used Support Vector Machine (SVM) for classification and trained the classifier with 1200 bacilli and 1200 non-bacilli pixels which were taken from the dataset images. They considered 30 features and used scalar feature selection method for determining the best one. They

### Table 3 – Comparative analysis with the method in [20].

| Key terms | Costafilho et al. [20] | Our proposed method |
| --- | --- | --- |
| No. of training samples | 1200 pixels belonging to bacilli and 1200 background pixels. | 1800 (900 bacilli images and 900 non-bacilli images) |
| Classifier | SVM | CNN |
| Recall (sensitivity) | 96.8% | 97.13% |
| Bacilli detection | Single bacilli only | Single bacilli and touching bacilli |
| Total no of bacilli considered for testing | 2456 | 1817 |
| Dataset | Costa et al. [27] | Costa et al. [27] |



| a | b | c |
| --- | --- | --- |
| d | e | f |
| g | h | i |

Fig. 5 – Segmentation and classification of TB bacilli. The first row (a), (b) and (c) shows the original input image. The images in the second row (d), (e) and (f) are final output. The objects in green boxes are bacillus and the objects in red box are non-bacillus objects. The last row (g), (h) and (i) are zoomed regions of (d), (e) and (f).

removed noise and artifacts by using three filters such as size filter, geometric filter, and rule-based filter. They looked only for single bacilli and since in our approach we considered both single and touching bacilli, our method has an edge over the method proposed in [20]. The details are given in Table 3.

## 5.    Conclusions

In this study, we present an automatic TB detection method based on CNN using microscopic sputum smear images. These methods can be incorporated into an automated microscope for detecting TB disease more accurately within a short duration than the manual detection. The proposed method was experimentally evaluated and got a sensitivity of 97.13%. In this paper, we also present a comparative study between the proposed method and existing method, where both of them use the same dataset. This automatic TB detection method can act as a companion to clinicians in the rural and urban areas of high TB burden countries where there is lack of properly trained technicians.

## Acknowledgment

REFERENCES

[1] Global tuberculosis report 2017, http://www.who.int/tb/publications/global_report/en/ [accessed 13.11.17].

[2] Priya E, Srinivasan S. Separation of overlapping bacilli in microscopic digital TB images. Biocybern Biomed Eng 2015;35:87–99.

[3] Panicker RO, Soman B, Saini G, Rajan J. A review of automatic methods based on image processing techniques for tuberculosis detection from microscopic sputum smear images. J Med Syst 2016;40(1):1–13.

[4] Chang J, Arbeláez P, Switz N, Reber C, Tapley A, Davis JL, et al. Automated tuberculosis diagnosis using fluorescence images from a mobile microscope. Proc. of Medical Image Computing and Computer-Assisted Intervention – MICCAI. 7512. 2012. pp. 345–52.

[5] Costa MG, Costa Filho CFF, Sena JF, Salem J, Lima MO. Automatic identification of *Mycobacterium tuberculosis* with conventional light microscopy. Proc. of 30th Annual International IEEE Eng Med Biol Soc; 2008. pp. 382–5.

[6] Sotaquir'a M, Rueda L, Narvaez R. Detection and quantification of bacilli and clusters present in sputum smear samples: a novel algorithm for pulmonary tuberculosis diagnosis. Proc. of International Conference on Digital Image Processing; 2009. pp. 117–21.

[7] Veropoulos K, Campbell C, Learmonth G, Knight B, Simpson J. The automated identification of tubercle bacilli using image processing and neural computing techniques. Proc.

[8] Veropoulos K, Campbell C, Learmonth G. Image processing and neural computing used in the diagnosis of tuberculosis. Proc. of IEE Colloquium on Intelligent Methods in Healthcare and Medical Applications (Digest No. 1998/514); 1998. 8/1-8/4.

[9] Khutlang R, Krishnan S, Whitelaw A, Douglas TS. Automated detection of tuberculosis in Ziehl-Neelsen stained sputum smears using two one-class classifiers. J Microsc 2010;237(1):96–102.

[10] Panicker RO, Soman B, Gangadharan KV, Sobhana NV. An adoption model describing clinician's acceptance of automated diagnostic system for tuberculosis. Health Technol 2016;10:1–11.

[11] Sadaphal P, Rao J, Comstock GW, Beg MF. Image processing techniques for identifying *Mycobacterium tuberculosis* in Ziehl-Neelsen stains. Int J Tuberc Lung Dis 2008;12(5):579–82.

[12] Makkapati V, Agrawal R, Acharya R. Segmentation and classification of tuberculosis bacilli from ZN-stained sputum smearimages. Proc. of IEEE International Conference on Automation Science and Engineering (CASE); 2009. pp. 217–20.

[13] Sotaquirá M, Rueda L, Narvaez R. Detection and quantification of bacilli and clusters present in sputum smear samples: a novel algorithm for pulmonary tuberculosis diagnosis. Proc. of International Conference on Digital Image Processing; 2009. pp. 117–21.

[14] Zhai Y, Liu Y, Zhou D, Liu S. Automatic Identification of *Mycobacterium tuberculosis* from ZN-stained sputum smear: algorithm and system design. Proc. of IEEE International Conference on Robotics and Biomimetics (ROBIO); 2010. pp. 41–6.

[15] Nayak R, Shenoy VP, Galigekere RR. A new algorithm for automatic assessment of the degree of TB-infection using images of ZN-stained sputum smear. Proc. of International Conference on Systems in Medicine and Biology (ICSMB); 2010. pp. 294–9.

[16] Khutlang R, Krishnan S, Dendere R, Whitelaw A, Veropoulos K, Learmonth G, et al. Classification of *Mycobacterium tuberculosis* in images of ZN stained sputum smears. IEEE Trans Inf Technol Biomed 2010;14(4):949–57.

[17] Costa Filho CFF, Costa MGF. Sputum Smear Microscopy for Tuberculosis: Evaluation of Autofocus Functions and Automatic Identification of Tuberculosis Mycobacterium. Understanding Tuberculosis – Global Experiences and Innovative Approaches to the Diagnosis, Dr. Pere-Joan Cardona (Ed.), ISBN: 978-953-307-938-7, InTech, pp. 277–292, 2012.

[18] Ayas S, Ekinci M. Random forest-based tuberculosis bacteria classification in images of ZN-stained sputum smear samples. SIViP 2010;8(1):49–61.

[19] Osman MK, Ahmad F, Saad Z, Mashor MY, Jaafar H. A genetic algorithm-neural network approach for *Mycobacterium tuberculosis* detection in Ziehl-Neelsen stained tissue slide images. Proc. of 10th International Conference on Intelligent Systems Design and Applications (ISDA). 2010. pp. 1229–34.

[20] Costa Filho CFF, Levy PC, Xavier CM, Fujimoto LBM, Costa MGF. Automatic identification of tuberculosis mycobacterium. Res Biomed Eng 2015;31(1):33–43.

[21] Chao Xu, Zhou D, Liu Y. Segmentation of touching *Mycobacterium tuberculosis* from Ziehl-Neelsen stained sputum smear images. Proc. of SPIE vol. 9812. 2015. pp. 981210–1.

[22] Ghosh P, Bhattacharjee D, Nasipuri M. A hybrid approach to diagnosis of tuberculosis from sputum. IEEE International

Conference on Electrical, Electronics, and Optimization Techniques (ICEEOT); 2016.

[23] Sergey I, Szegedy C. Batch normalization: accelerating deep network training by reducing internal covariate shift. ICML'15 Proceedings of the 32nd International Conference on Machine Learning – vol. 37; 2015. p. 448–56.

[24] Krizhevsky A, Sutskever I, Hinton GE. ImageNet classification with deep convolutional neural networks. Proceedings of the 25th International Conference on Neural Information Processing Systems – Vol. 1; 2012. p. 1097–105.

[25] Glorot X, Bengio Y. Understanding the difficulty of training deep feed forward neural networks. Proceedings of the Thirteenth International Conference on Artificial Intelligence and Statistics (AISTATS). Vol. 9; 2010. p. 249–56.

[26] LeCun Y, Bottou L, Orr G, Muller K. Efficient backprop. Neural Networks: Tricks of the trade. LNCS 1524. Springer; 1998, ISBN 978-3-540-65311-0.

[27] Costa MG, Costa Filho CFF, Junior KA, Levy PC, Xavier CM, Fujimoto LB. A sputum smear microscopy image database for automatic bacilli detection in conventional microscopy. Proc. of 36th Annual International Conference of IEEE Engineering in Medicine and Biology Society (EMBC). 2014. pp. 2841–4.

[28] López YP, Costa Filho CFF, Aguilera LMR, Costa MGF. Automatic classification of light field smear microscopy patches using Convolutional Neural Networks for identifying Mycobacterium Tuberculosis. Proceedings of 2017 CHILEAN Conference on Electrical, Electronics Engineering, Information and Communication Technologies (CHILECON); 2017.

[29] Froment J. Parameter-free fast pixel wise non-local means denoising. Image Process On Line 2014;4:300–26.

[30] Otsu N. A threshold selection method from gray-level histograms. Automatica 1975;11:23–7.

[31] Goodfellow I, Bengio Y, Courville A, editors. Deep learning. London: The MIT Press; 2016.

[32] CostaFilho CFF, Levy PC, Xavier M, Costa MGF, Fujimoto LBM, Salem J. Micobacterium tuberculosis recognition with conventional microscopy. Proceedings of 34th Annual International IEEE Engineering in Medicine and Biology Society Conference; 2012. p. 6263–8.